PHYSICAL REVIEW B VOLUME 43, NUMBER 14 15 MAY 1991-I

Satellite structure in the photoemission spectra of MnO(100)

Shin-Puu Jeng
Surface Science Laboratory, Department of Applied Physics, Yale University, New Haven, Connecticut 06520

Robert J. Lad
Department of Physics, University of Maine, Orono, Maine 04469

Victor E. Henrich
Surface Science Laboratory, Department of Applied Physics, Yale University, New Haven, Connecticut 06520

(Received 6 August 1990; revised manuscript received 26 December 1990)

The satellite structure in both core-level and valence-band photoemission spectra from single-crystal MnO(100) has been studied by using both x-ray photoemission spectra and resonant photoemission. Only very weak satellites are present in the Mn $2p$ core-level spectra, while no satellite structure is evident in the Mn $3p$ and $3s$ core-level spectra. The small intensity of the satellite peaks in MnO is consistent with the trend predicted by a recent ligand charge-transfer screening model; such screening is quite weak in MnO in comparison to the heavier transition-metal oxides. The valence-band spectrum, however, exhibits a stronger satellite peak than predicted by the model, and its origin has been uncertain. We have found that, while the satellite in the valence-band spectrum can be resonantly enhanced across the Mn $3p \rightarrow 3d$ optical excitation threshold, its intensity depends strongly upon surface treatment. The satellite disappears with only 0.2–1-langmuir exposure of oxygen at 340 °C, confirming that it is essentially a surface-related feature. We suggest that it is associated with point defects on the surface, presumably surface Mn vacancies.

I. INTRODUCTION

The interpretation of so-called "satellite" features in photoemission spectra, which are generally less intense features occurring at several eV higher binding energy than the "main" lines that are expected in the spectra based upon a one-electron picture of the electronic structure of the material, has been the subject of lively debate for decades. These satellites are visible in both the core-level and valence-band photoemission spectra from a wide variety of materials. For some materials their interpretation is straightforward (e.g., plasmon satellites in nearly-free-electron materials), but for transition-metal compounds these satellites are still not well understood.[1] The origin of the various features in the photoelectron (and other) spectra of transition-metal compounds has recently been discussed by Sawatzky and co-workers,[2–4] and we will use their notation in this paper. In the heavy transition-metal compounds ($Z > 25$), satellites occur at binding energies between 5 and 7 eV greater than the main lines and have recently been ascribed to multielectron effects involving the transition-metal $3d$ and ligand p states.[1–9] Consider core-hole formation in a heavy $3d$ transition-metal oxide having a

$$\alpha 3d^n + \beta 3d^{n+1}\underline{L} + \gamma 3d^{n+2}\underline{L}^2$$

ground state configuration, where $\underline{L}$ and $\underline{L}^2$ denote one and two holes in the ligand p states, respectively; the normal configuration for the ligands is $O^{2-}\ 2p^6$. For predominantly ionically bonded materials, α is the largest coefficient in the ground state. After emission of an electron from the core level, the final state of the system can be described by

$$\alpha' \underline{c} 3d^n + \beta' \underline{c} 3d^{n+1}\underline{L} + \gamma' \underline{c} 3d^{n+2}\underline{L}^2 ,$$

where $\underline{c}$ denotes a cation core hole. If the effective core-hole–d-electron Coulomb attraction energy (Q) is large, then, after creation of the core hole, the energy of the system can be lowered by electron transfer from the ligand orbitals into the cation $3d$ orbitals. In that case the largest coefficient in the final state will be β', and the main line in the core-level photoemission from these compounds can be assigned to a well-screened $\underline{c} 3d^{n+1}\underline{L}$ configuration. The satellite then corresponds to a poorly screened $\underline{c} 3d^n$ final state.[2–5] The assignment of satellites in valence-band photoemission, where the final-state configuration is

$$\alpha'' 3d^{n-1} + \beta'' 3d^n\underline{L} + \gamma'' 3d^{n+1}\underline{L}^2 ,$$

is less obvious, since the Coulomb interaction due to the $3d$ hole created by photoionization is not strong enough to widely separate different final-state configurations.[4] However, if a mechanism analogous to that discussed above for core-hole formation is assumed to apply, the main line and satellite configurations can be regarded as $3d^n\underline{L}$ and $3d^{n-1}$, respectively.[4,6–8]

For the light transition-metal compounds ($Z < 25$), the dominant screening mechanisms are quite different; models such as exciton creation have been proposed to explain the satellites which occur at binding energies higher than those expected for charge-transfer satellites.[10] While the interpretation of the satellite structure in the

heavy transition-metal oxides is in good agreement with their bulk optical properties, a good understanding of the dominant screening processes for light transition-metal compounds is still lacking.[4]

Manganese oxide (MnO; $Z=25$) is a conceptually simple rocksalt monoxide since the large exchange splitting of the Mn ($3d^5$) ion separates the $3d$ level into occupied spin-up and empty spin-down components.[11] Compared to Ni, Co, and Fe monoxides, MnO has a relatively large charge-transfer energy (Δ) and a relatively small d-d Coulomb repulsion energy (U), and thus it is of a more ionic nature.[5,7] The satellite structure of MnO is particularly interesting because MnO is at the border between the light and heavy $3d$ transition-metal oxides. The study of its satellite structure may assist our understanding of the difference between the dominant screening mechanisms of heavy and light transition-metal oxides.

In previous studies[12–14] (including our own) a satellite feature was observed in the valence-band spectrum of MnO, but the origin of the satellite (i.e., whether it represents the bulk properties of MnO) was questioned.[7,12] We have thus measured both core-level and valence-band photoemission spectra on cleaved single crystal MnO(100) using synchrotron radiation, He II and Al $K\alpha$ x-ray sources as a function of sample preparation and surface treatment. Based upon the changes of the satellite structure with photon energy and surface treatment, we suggest that the satellite in the valence-band spectrum is actually a surface-related feature and does not originate from the bulk electronic structure of MnO.

II. EXPERIMENTAL PROCEDURE

A single crystal of MnO obtained from Crystal Tec (Grenoble, France) was oriented and cut into rods of 4×4 mm^2 cross section having the (100) face normal to the rod axis. The sides of these cleavage rods were coated with ~0.5 μm of Pd-Au alloy in order to reduce charging during photoemission measurements; however, uncoated cleavage rods were also used in some experiments. Although the single crystal exhibited high-quality Laue x-ray diffraction patters, x-ray diffractometer analysis revealed that the sample contained ≤7 mol % of Mn_3O_4. The MnO(100) surface was produced by cleaving the sample *in situ* in the surface analysis system at a base pressure below 2×10^{-10} Torr. In order to measure the changes in photoemission spectra at elevated temperatures, a thin slice of MnO(100) was cut from the same boule as the cleavage rods and polished successively to a 0.25 μm diamond paste finish. The polished MnO(100) was mounted onto a tantalum holder and heated by a tungsten filament mounted behind the sample. To monitor the temperature, a chromel-alumel thermocouple was spot-welded to the tantalum holder in contact with MnO crystal. The MnO crystal was carefully cleaned by a cyclic sputter-annealing process until no impurities could be detected by Auger electron spectroscopy. A small amount of steady-state charging occurred during photoemission at room temperature on the MnO surface; thus spectra are plotted on a relative-binding-energy scale. No charging effects were observed at elevated temperature (≥70 °C) due to thermally activated conductivity.[15,16]

Photoemission spectra were obtained with both unpolarized 40.8-eV photons from a helium dc discharge lamp and 1486.6-eV photons from an Al anode x-ray source in our laboratory. These spectra were recorded with a Physical Electronics 15-255G double-pass cylindrical-mirror analyzer (CMA) whose axis was normal to the sample surface. The resonant photoemission experiments were performed on a beamline U14 at the National Synchrotron Light Source, Brookhaven National Laboratory. Angle-integrated photoemission spectra were also measured with a double-pass CMA of the same model as in the fixed photon-energy experiments. The CMA axis was oriented 45° to the (100) surface, and photons were incident at an angle of 45° to the (100) surface normal. For each spectrum in which the photon energy was varied, the photocurrent of a Ni diode flux monitor was used to correct for variations in light intensity from the monochromator.

III. RESULTS

A. X-ray photoelectron spectra

The XPS photoemission spectra of Mn $2p_{3/2}$, $2p_{1/2}$, and $3p$ core levels and the valence band from vacuum-cleaved MnO(100) measured using Al $K\alpha$ x rays are compared in Fig. 1. In order to directly compare the satellite structure in different spectra, the spectra have been

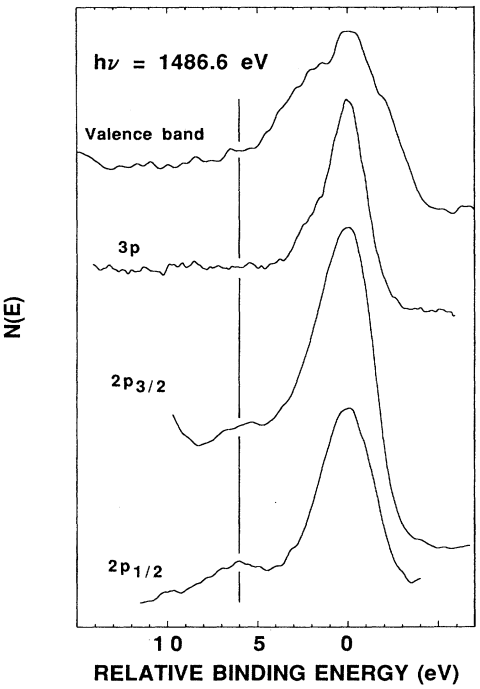

FIG. 1. XPS spectra from UHV cleaved MnO(100) showing the satellite location with respect to the main core-level and valence-band photoemission peaks. $h\nu=1486.6$ eV.

aligned with their main lines centered at 0 eV relative binding energy. Weak but distinct satellites are observed at a binding energy about 6 eV higher than the main lines in the Mn $2p$ core-level spectra, whereas no evident satellites are observed in the Mn $3p$ core-level or the valence-band spectra. (Although the XPS $3s$ core-level spectrum is not shown here, an $\sim$6-eV exchange splitting was obtained on uncoated cleavage rods, in contrast to the previously reported smaller splitting.[13])

B. Ultraviolet and resonant photoemission

Although no evident satellite structure is observed in the XPS valence-band spectrum shown in Fig. 1, our previous ultraviolet photoemission spectroscopy (UPS) study of MnO has shown substantial photoemission intensity at a binding energy of $\sim$7 eV higher than the main line in the valence-band spectra.[13] The discrepancy can be clearly seen in Fig. 2, in which both UPS and XPS valence-band spectra from a cleaved MnO(100) crystal are compared. [The spectra are aligned at the maxima of the largest emission peak; emission appears to extend into the band gap in the 1486.6-eV spectrum due to the much poorer resolution (about 1 eV) at that photon energy.] Although the amplitude of the satellite was found to be somewhat sample dependent, a satellite in the UPS spectrum from a cleaved MnO(100) surface clearly exists. (The possibility of this satellite being due to contamination from either CO or H_2O chemisorption on MnO can be ruled out because of the short data acquisition time and low base pressure in the vacuum chamber throughout the analysis.)

When the photon energy is varied across the region of the Mn $3p \rightarrow 3d$ optical absorption edge, we find that both the satellite and other features in the UPS spectra are resonantly enhanced. This resonance arises from the interference between the direct emission of $3d$ electrons ($3d^n + h\nu \rightarrow 3d^{n-1} + e^-$) and the $3p \rightarrow 3d$ excitation ($3p^6 3d^n + h\nu \rightarrow [3p^5 3d^{n+1}]^*$) followed by a super-Coster-Kronig decay ($[3p^5 3d^{n+1}]^* \rightarrow 3p^6 3d^{n-1} + e^-$).[1] Figure 3 shows the valence-band spectra of cleaved MnO(100) as a function of photon energy, in which both the main lines and the satellite are enhanced simultaneously relative to the nonresonant O $2p$ emission as the photon energy is varied across the $3p \rightarrow 3d$ excitation threshold at $\sim$51 eV.

C. Effect of surface treatment

The intensity of the satellite emission in MnO(100) is found to depend strongly upon the way in which the surface is treated. As shown in Fig. 4, the intensity of the satellite decreases upon Ar^+-ion bombardment [Fig. 4(b)], compared to the cleaved surface [Fig. 4(a)], while it regains some of its intensity after the MnO sample is heated to 340 °C [Fig. 4(c)]. Moreover, the intensity of the satellite is strongly affected by exposure to minute amounts of oxygen. As shown in Figs. 4(d) and 4(e), the satellite disappears after only 0.2–1 L of oxygen exposure at 340 °C, while the other features in the valence-band photoemission spectrum remain virtually unaffected. The

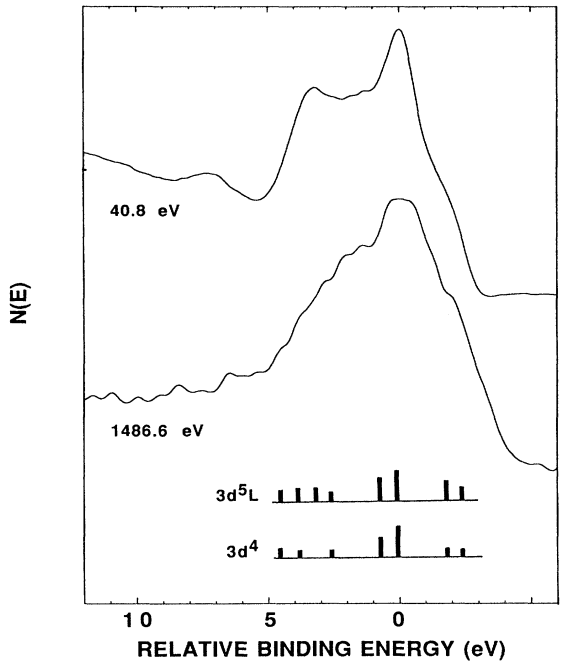

FIG. 2. XPS and UPS valence-band photoemission spectra taken on UHV cleaved MnO(100). The spectra are compared to calculated $3d^4$ and $3d^5\underline{L}$ final-state intensities from a CI calculation for a $(MnO_6)^{10-}$ cluster (Refs. 7 and 12).

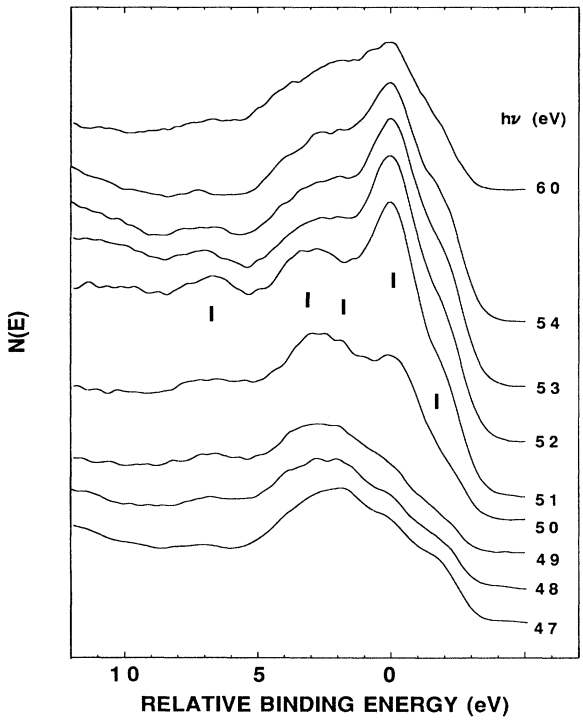

FIG. 3. Angle-integrated EDC's measured from cleaved MnO(100) showing resonant enhancement of the $3d$ states.

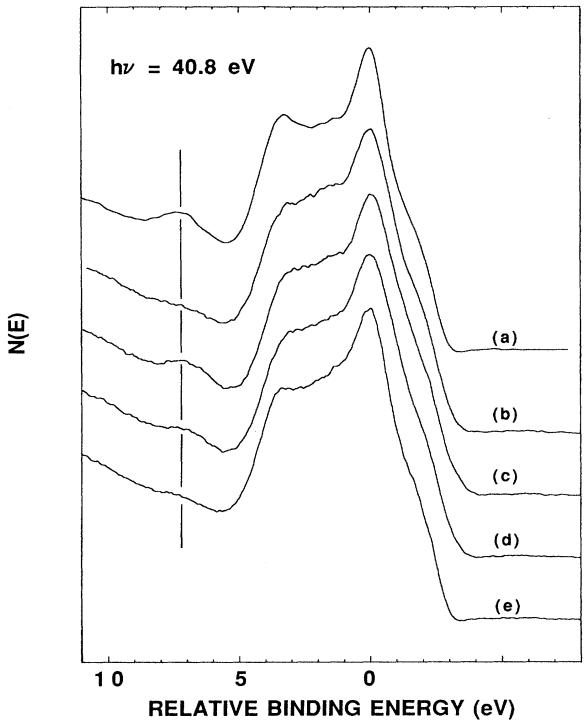

FIG. 4. UPS spectra from MnO(100) for (a) cleaved in UHV, (b) then bombarded with 2-keV Ar^+ ions, (c) then heated at 340 °C, (d) then exposed to 0.2 L of oxygen at 340 °C, and (e) further exposed to 1 L of oxygen at 340 °C. $h\nu = 40.8$ eV.

low dosage of oxygen required to suppress the satellite rules out the possibility that the MnO surface is being oxidized to a higher valency oxide. In contrast to such a striking surface sensitivity for the satellite in the valence-band spectrum, the $2p$ core-level spectra from a cleaved MnO surface, shown in Fig. 5, are unchanged even after the surface is bombarded with Ar^+ ions at room temperature.

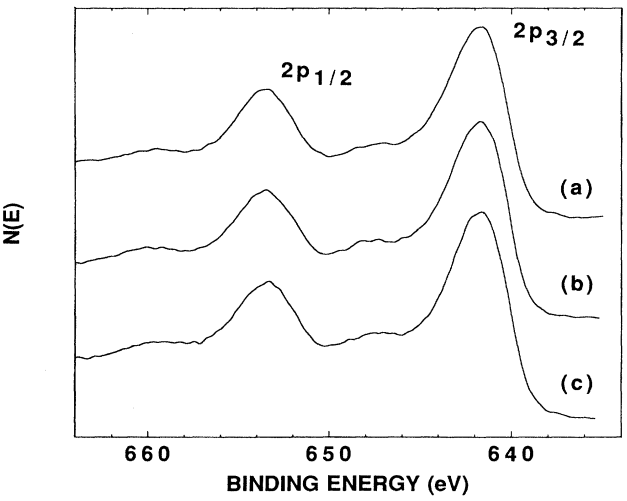

FIG. 5. Mn $2p$ XPS spectra from MnO(100) as a function of surface treatment: (a) cleaved in UHV, (b) bombarded with 2-keV Ar^+ ions, and (c) then heated at 340 °C.

IV. DISCUSSION

A. Origin of satellites in photoelectron spectra

As has been shown for transition-metal dihalide compounds, both the ratio of the intensity of the satellite to that of the main peaks in core-level spectra and their binding energy splitting can be properly described within the cluster approximation in terms of the fundamental parameters Δ, U, Q, and T (the ligand p-metal d-transfer integral).[2–5,9] Upon the creation of a core-hole, the interaction with the core hole lowers the energy of the valence-electron configuration.[2–5] The energies of the main lines and the satellites in the core-level spectrum are determined by the differences between the energies of the d^n, $d^{n+1}\underline{L}$, and $d^{n+2}\underline{L}^2$ valence electronic configurations in the initial state and the $\underline{c}d^n$, $\underline{c}d^{n+1}\underline{L}$, and $\underline{c}d^{n+2}\underline{L}^2$ configurations in the final state. If the interaction between the core hole and valence electrons is large enough, the energy of the system can be lowered by a charge transfer from the ligand orbitals into the d orbitals, thus modifying the level sequence of valence-state configurations.[3] The $\underline{c}d^{n+1}\underline{L}$ configuration will have the largest final-state energy (i.e., the lowest binding energy) and thus corresponds to the main line, while the satellite corresponds to either a $\underline{c}d^n$ or a $\underline{c}d^{n+2}\underline{L}^2$ final state having a higher binding energy. If such a Coulomb interaction is very strong, the fully relaxed $\underline{c}d^{n+2}\underline{L}^2$ final state will eventually become the main line.[3] In the same spirit, based upon a molecular-orbital model by Asada and Sugano,[17] Hüfner *et al.*[18] also presented a simple charge-transfer screening criterion for the ionic transition-metal compounds. Namely, charge-transfer satellites will be present in the core-level spectra if $Q > \Delta$. For the case where $Q < \Delta$, no inversion of the valence-electronic configuration will occur; consequently no core-hole induced charge-transfer satellites will be seen in the spectra.

In transition-metal compounds, the intensity ratio of the satellite to the main peak is a function of the atomic parameters Q, U, T, and Δ.[3,5] When comparing the intensities of satellites associated with different core levels on the same ion, such as $2p$ and $3p$, the parameter that will vary the most is Q, the core-hole–d-electron Coulomb attraction, since Δ depends only on the ligands adjacent to the cation, T depends only on the hybridization between ligand and metal $3d$ levels, and U involves only the d-d Coulomb interaction. The ratio of the satellite to the main peaks is found to increase with increasing Q, as shown in Fig. 3 of Ref. 3. Thus the XPS spectra in Fig. 1 suggest that Q is larger for the Mn $2p$ core level than it is for the $3p$. The absence of a satellite in the $3p$ core-level spectrum is in agreement with such a trend; a recent study of atomic Mn and Mn ionic compounds showed that outer core-level spectra are of unscreened intra-atomic nature.[19] Consistent with the fact that MnO is a strongly ionic compound having a large Δ, the intensity ratio of the satellite and main peaks in the $2p_{3/2}$

core-level spectrum is low; the ratio is ~ 0.06, which is close to that of MnF_2.[5] This small value suggests that MnO lies on the borderline between charge transfer and other screening mechanisms.

The valence band XPS and UPS spectra can be compared with the results of recent configuration-interaction calculations. Fujimori *et al.*[7,12] have previously interpreted the valence-band features of MnO within the configuration-interaction (CI) picture considering the hybridization of $3d^4$ and $3d^5\underline{L}$ final states; the $3d$-derived main lines are attributed to a strong hybridization of the $3d^4$ and the $3d^5\underline{L}$ final states, with more $3d^5\underline{L}$ spectral weight. The CI result is included in Fig. 2; note that the calculation does not show any high binding energy satellite emission.

In our previous photoemission study of MnO,[13] the satellite was thought to be due predominantly to a $3d^4$ final state emission, with the main lines due to $3d^5\underline{L}$ final-state emission. In the present study, we find that these assignments are not consistent with the photon-energy-dependent behavior (UPS versus XPS) shown in Fig. 2. Since the charge-transfer process depends upon the response time of the medium,[20,21] the $3d^5\underline{L}$ adiabatic peak is expected to gain more spectral weight as the sudden approximation is relaxed at low photon energies (i.e., when the photoemitted electrons remain in the vicinity of the excited ion for a relative long time), while the $3d^4$ unscreened peak is expected to increase with respect to the $3d^5\underline{L}$ peak as the photon energy increases. Such a photon-energy dependence has been clearly seen in other heavier transition-metal oxides.[22–25] For example, the main lines in the valence-band spectrum of NiO are attributed to a $3d^8\underline{L}$ final state and the satellite to a $3d^7$ final state.[4,6,7] The satellite is very prominent in the XPS spectrum, whereas its intensity decreases with respect to the main line as the photon energy decreases in UPS,[22–24] the intensity of the NiO satellite decreases to such an extent that it is even not visible in the spectrum taken at photon energy of 40.8 eV.[23] Thus the photon-energy dependence of the MnO satellite observed in Fig. 2 is clearly different than that expected for a $3d^4$ final state.

B. Resonant photoemission from transition-metal compounds

As has been demonstrated for Fe, Ni, and Cu compounds, the intensity of the $3d^{n-1}$ final-state features generally exhibits a strong Fano-type resonance near the $3p \rightarrow 3d$ threshold as the photon energy is varied in constant-initial-state (CIS) photoemission spectra, while the resonance for a $3d^n\underline{L}$ final state is relatively weak and exhibits an antiresonant dip (rather than a peak) on the lower photon-energy side in its CIS spectrum.[6,24–26] The main line in the MnO valence band was previously assigned to a $3d^5\underline{L}$ final state and the satellite to a $3d^4$ final state.[13] However, the resonant enhancement of the main lines in MnO spectra suggests that they contain significant $3d^{n-1}$ final-state spectral weights, in contrast to the main lines for heavier transition-metal oxides which have more distinct $3d^n\underline{L}$ final-state character.[6,24–26] The distribution of the $3d$-derived features (including the contribution from both surface and bulk) across the valence band can be seen clearly in the difference spectrum in Fig. 6, which is taken between photoemission spectra just above and just below the $3p \rightarrow 3d$ resonance; the difference spectrum removes most of the unhybridized O $2p$ contribution from the spectrum. The increase of hybridization between $3d^{n-1}$ and $3d^n\underline{L}$ final states in the $(n-1)$ particle state is expected due to the smaller U and larger Δ as one moves from the heavier monoxides to MnO; such a trend can also be seen in the CI calculation by Fujimore *et al.*[7,12] Thus the $3p \rightarrow 3d$ resonant enhancement of the satellite suggests that it is clearly associated with Mn cations.

C. Surface nature of the valence-band satellite in MnO

Although resonant photoemission spectra show that the satellite in MnO is associated with the Mn cations, its behavior is not consistent with an explanation in terms of bulk electronic structure. The spectra in Fig. 4 clearly show that the satellite is a surface-related feature. The absence of any satellite in XPS valence-band spectra in Figs. 1 and 2 is also consistent with this picture. The escape depth of photoelectrons having kinetic energies near 1400 eV, as in the XPS valence-band spectra, is much longer than that for electrons excited by photons in the range of 30–80 eV. Thus a satellite of surface origin should be much weaker in XPS spectra, where tens of angstroms of material are being sampled, than in UPS spectra where the electron mean free path is a few angstroms.

Although the intensity of the valence-band satellite in Fig. 4 exhibits a complex dependence on surface treatment, decreasing under both ion bombardment and O_2 exposure while increasing at higher temperature, it is probable that the satellite is associated with surface de-

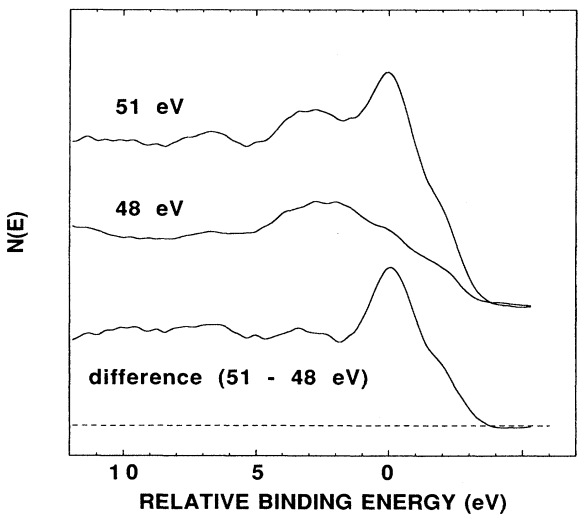

FIG. 6. Angle-integrated EDC's from cleaved MnO(100) for photon energies of 48 and 51 eV and the difference between them, which reflects primarily the energy distribution of the $3d$-derived final state.

fects. The presence of a high density of defects on cleaved MnO(100) is supported in part by the high reactivity of cleaved MnO(100) for chemisorption of various gases at room temperature.[27] Two categories of defects are likely to be present on a cleaved single-crystal oxide surface: point defects such as vacancies and adatoms, and extended defects including steps, kinks, and edges.[28] Since the valence-band satellite in MnO(100) occurs at several eV higher binding energy than the main lines, it is most likely associated with a decrease in the $3d$-electron population on Mn cations at surface defect sites (i.e., holes on the Mn cations); any increase in the $3d$-electron population on Mn ions at defects should result in features in the photoemission spectra at lower binding energy, as has been observed for NiO,[23] CoO,[29] TiO_2,[30] etc. It is instructive to compare the MnO valence-band photoemission satellite with the 9.5-eV satellite in the valence-band spectra obtained from $YBa_2Cu_3O_{7-x}$ superconductors, since the 9.5-eV satellite there is known to be a surface-related feature arising from either a surface phase transformation, surface defects, or impurity phases in the crystals.[31,32] Oxygen $2p$ holes are present in the $YBa_2Cu_3O_{7-x}$ crystals for $x<0.5$, and the origin of the 9.5-eV satellite has been interpreted as an oxygen satellite arising from the Coulomb correlation of the $2p$ hole created on an O anion during the photoemission process and an O $2p$ hole on a neighboring O site.[33] While this interpretation has been subject to some dispute,[32] it is supported by the resonant enhancement of the 9.5-eV satellite across the O $2s \rightarrow 2p$ excitation threshold.[34] Recent theoretical work[35] on models of several transition-metal oxides has suggested that holes in MnO tend to be localized on the metal sites, in contrast to the Cu-oxide–based superconductors whose holes are mainly associated with oxygen sites. Since the satellite in MnO is resonantly enhanced by the Mn $3p \rightarrow 3d$ excitation, the high binding energy satellite in the MnO valence-band photoemission spectrum could thus result from an additional Coulomb attraction between the photoemitted $3d$ electron and a defect-induced hole on a Mn site (presumably corresponding to Mn surface vacancies). Further experimental and theoretical work is certainly necessary in order to clarify this point.

D. Possible effect of bulk defects

Since the valence-band satellite is observed even in the spectrum obtained from vacuum-cleaved MnO(100), we must consider the possible effect of bulk defects. Two types of bulk imperfections, a Mn_3O_4 secondary phase and Mn vacancies, are known to exist in MnO.[36,37] Small amounts of Mn_3O_4 are commonly found in commercial MnO single crystals,[37] as is the case here. Because the amount of Mn_3O_4 in the crystal is only a few percent, the presence of this secondary phase is probably too small to be discernable in the photoemission spectra of MnO. For the second type of imperfection, recent studies suggest that a substantial number of cation vacancies can exist in MnO; the nonstoichiometric $Mn_{1-x}O$ can have x between 0.001 and 0.15 similar to wustite $Fe_{1-x}O$.[36] However, the bulk concentration of Mn vacancies in MnO should not be large enough, as suggested by its insulating nature at room temperature, to markedly affect the MnO photoemission spectra. Moreover, neither the Mn_3O_4 secondary phase nor Mn vacancies in the bulk can explain the surface sensitivity of the satellite shown in Figs. 2 and 3. Therefore imperfections in bulk MnO are unlikely to be the only origin for the satellite.

V. SUMMARY

Both XPS and resonant photoemission have been used to study the core-level and valence-band satellite structure in single-crystal MnO(100). The very small amplitude of the satellites associated with the Mn $2p$ core level and the absence of satellites in the $3s$ and $3p$ core-level spectra are consistent with the predictions of a recent ligand charge-transfer screening model. The valence-band photoemission spectra, however, contains a relatively strong satellite feature which exhibits resonant behavior as the photon energy is tuned through the Mn $3p \rightarrow 3d$ optical excitation threshold; this satellite is not predicted by the model. Its amplitude is found to be highly dependent upon surface treatment, and we suggest that it is associated with point defects on the surface; its resonant behavior indicates that it may correspond to excitations at surface Mn vacancies.

ACKNOWLEDGMENTS

The authors would like to thank the staff of National Synchrotron Light Source for helpful technical assistance and Dr. R. L. Kurtz for stimulating discussions. This work was partially supported by National Science Foundation Solid State Chemistry Grant No. DMR-87-11423.

[1]L. C. Davis, J. Appl. Phys. **59**, R25 (1986), and references therein.

[2]G. van der Laan, C. Westra, C. Haas, and G. A. Sawatzky, Phys. Rev. B **23**, 4369 (1981).

[3]J. Zaanen, C. Westra, and G. A. Sawatzky, Phys. Rev. B **33**, 8060 (1986).

[4]G. A. Sawatzky, in *Core-Level Spectroscopy in Condensed Systems,* edited by J. Kanamori and A. Kotani (Springer-Verlag, Berlin, 1988), p. 99.

[5]J. Park, S. Ryu, M. Han, and S. J. Oh, Phys. Rev. B **37**, 10 867 (1988).

[6]A. Fujimori and F. Minami, Phys. Rev. B **30**, 957 (1984); A. Fujimori, F. Minami, and S. Sugano, *ibid.* **29**, 5225 (1984).

[7]A. Fujimori, in *Core-Level Spectroscopy in Condensed Systems* (Ref. 4), p. 136.

[8]G. A. Sawatzky and J. W. Allen, Phys. Rev. Lett. **53**, 2239 (1984).

[9]D. E. Ramaker, J. Electron Spectrosc. Relat. Phenom. **52**, 341

(1990).
[10]D. K. G. deBoer, C. Haas, and G. A. Sawatzky, Phys. Rev. B **31**, 4401 (1984).
[11]J. B. Goodenough, Prog. Solid State Chem. **5**, 268 (1972).
[12]A. Fujimori, N. Kimizuka, T. Akahane, T. Chiba, S. Kimura, F. Minami, K. Siratori, M. Taniguchi, S. Ogawa, and S. Suga, Phys. Rev. B **42**, 7580 (1990); A. Fujimori, N. Kimizuka, M. Saeki, S. Kimura, F. Minami, T. Akahane, T. Chiba, K. Siratori, M. Taniguchi, S. Ogawa, and S. Suga, Institute for Solid State Physics Synchrotron Radiation Laboratory Activity Report, 1986, p. 53 (unpublished).
[13]R. J. Lad and V. E. Henrich, Phys. Rev. B **38**, 10 860 (1988).
[14]D. E. Eastman and J. L. Freeouf, Phys. Rev. Lett. **34**, 395 (1975).
[15]M. A. Langell and N. R. Cameron, Surf. Sci. **185**, 105 (1987).
[16]J. E. Keem, J. M. Honig, and L. L. Van Zandt, Philos. Mag. **37**, 537 (1978).
[17]S. Asada and S. Sugano, J. Phys. Soc. Jpn. **41**, 1291 (1976).
[18]S. Hüfner, Solid State Commun. **47**, 943 (1983); V. Kinsinger, I. Sander, P. Steiner, R. Zimmerman, and S. Hüfner, *ibid.* **73**, 527 (1990). The separation between d^n and $d^{n+1}\underline{L}$ is Δ, i.e., E_g (optical energy gap) in Hüfner's paper.
[19]B. Hermsmerier, J. Osterwalder, D. J. Friedman, and C. S. Fadley, Phys. Rev. Lett. **62**, 478 (1989); B. Hermsmerier, C. S. Fadley, M. O. Kraus, J. Jimenez-Mier, P. Gerard, and S. T. Manson, *ibid.* **61**, 478 (1988).
[20]G. A. Sawatzky and A. Lenselink, J. Chem. Phys. **72**, 3748 (1980).
[21]J. W. Gadzuk and M. Sunjic, Phys. Rev. B **12**, 524 (1975).
[22]D. E. Eastman and J. L. Freeouf, Phys. Rev. Lett. **34**, 395 (1975).
[23]J. M. McKay and V. E. Henrich, Phys. Rev. Lett. **53**, 2343 (1984); Phys. Rev. B **32**, 6764 (1985).
[24]S. J. Oh, J. W. Allen, I. Lindau, and J. C. Mikkelsen, Phys. Rev. B **26**, 4845 (1982).
[25]A. J. Fujimori, M. Saeki, N. Kimizuka, M. Taniguchi, and S. Suga, Phys. Rev. B **34**, 7138 (1986); G. van der Laan, Solid State Commun. **42**, 165 (1982).
[26]L. C. Davis, Phys. Rev. B **25**, 2912 (1982); A. Fujimori, N. Kimizuka, M. Taniguchi, and S. Suga, *ibid.* **36**, 6691 (1987); A. Kakizaki, K. Sugeno, T. Ishii, H. Sugawara, I. Nagakura, and S. Shin, *ibid.* **28**, 1026 (1983); R. J. Lad and V. E. Henrich, *ibid.* **39**, 13 478 (1989); M. R. Thuler, R. L. Benbow, and Z. Hurych, *ibid.* **27**, 2082 (1983).
[27]R. J. Lad and V. E. Henrich, J. Vac. Sci. Technol. A **6**, 781 (1988).
[28]V. E. Henrich, Rep. Prog. Phys. **48**, 1481 (1985).
[29]J. Mackay and V. E. Henrich, Phys. Rev. B **39**, 6156 (1989); S.-P. Jeng and V. E. Henrich, Solid State Commun. **75**, 1013 (1990).
[30]V. E. Henrich, G. Dresselhaus, and H. J. Zeiger, Phys. Rev. Lett. **36**, 1335 (1976); Z. Zhang, S.-P. Jeng, and V. E. Henrich, Phys. Rev. B **43**, 12 004 (1991).
[31]A. J. Arko, R. S. List, R. J. Bartlett, S.-W. Cheong, Z. Fisk, J. D. Thompson, C. G. Olson, A.-B. Yang, R. Liu, C. Gu, B. W. Veal, J. Z. Liu, A. P. Paulikas, K. Vandervoort, H. Claus, J. C. Campuzano, J. E. Schirber, and N. D. Shinn, Phys. Rev. B **40**, 2268 (1989); R. S. List, A. J. Arko, Z. Fisk, S.-W. Cheong, S. D. Conradson, J. D. Thompson, C. B. Pierce, D. E. Peterson, R. J. Bartlett, N. D. Shinn, J. E. Shirber, B. W. Veal, A. P. Paulikas, and J. C. Campuzano, *ibid.* **38**, 11 966 (1988).
[32]D. E. Fowler, C. R. Brundle, J. Lerczak, and F. Holtzberg, J. Electron Spectrosc. Relat. Phenom. **52**, 323 (1990).
[33]D. E. Ramaker, Phys. Rev. B **38**, 11 816 (1988).
[34]R. L. Kurtz, S. W. Robey, R. L. Stockbauer, D. Mueller, A. Shih, and L. Toth, Phys. Rev. B **39**, 4768 (1988).
[35]K. Yamaguchi, M. Nakano, H. Namimoto, and T. Fueno, Jpn. J. Appl. Phys. **28**, L479 (1989); **27**, L1835 (1988).
[36]R. W. Grimes, A. B. Anderson, and A. H. Heuer, J. Phys. Chem. Solids, **48**, 45 (1987); M. Radler, J. Faber, and J. B. Cohen, Proc. Mater. Res. Soc. Symp. **138** (1988); M. Keller and R. Dieckmann, Ber. Bunsenges. Phys. Chem. **89**, 883 (1985).
[37]M. S. Jagadeesh and M. S. Seehra, Phys. Rev. B **21**, 2897 (1980); S. Mochizuki, B. Pirious, and J. Dexpert-Ghys, J. Phys. Condens. Matter **2**, 5225 (1990).